HEAVY VECTOR MESON PHOTOPRODUCTION IN ULTRA-PERIPHERAL COLLISIONS AT THE LHC*

Evgeny Kryshen

National Research Center "Kurchatov Institute"
Petersburg Nuclear Physics Institute (PNPI), Gatchina, 188300, Russia

(Received April 9, 2019)

Pb nuclei, accelerated at the LHC, are sources of strong electromagnetic fields that can be used to measure photon-induced interactions in a new kinematic regime. These interactions can be studied in ultra-peripheral p–Pb and Pb–Pb collisions where impact parameters are larger than the sum of nuclear radii and hadronic interactions are strongly suppressed. Heavy quarkonium photoproduction is of particular interest since it is sensitive to gluon distributions in target hadrons. An overview of recent results on heavy vector meson photoproduction in ultra-peripheral Pb–Pb collisions and p–Pb collisions at the LHC will be presented, and implications for the study of gluon density distributions and nuclear gluon shadowing will be discussed. In addition, projections for heavy vector meson photoproduction measurements in LHC Run 3 and 4 will be presented.

DOI:10.5506/APhysPolB.50.1095

1. Introduction

Lead nuclei, accelerated at the LHC, are sources of strong electromagnetic fields, which are equivalent to a flux of quasi-real photons, thus p–Pb and Pb–Pb collisions can be used to measure γp and γPb interactions in a new kinematic regime. These interactions are usually studied in ultra-peripheral collisions (UPC), characterized by impact parameters larger than the sum of the radii of the incoming hadrons, in which hadronic interactions are strongly suppressed [1, 2].

Heavy vector meson photoproduction measurements in ultra-peripheral collisions at the LHC are of particular interest allowing one to probe poorly known gluon distributions at low x and search for gluon saturation effects because, in the pQCD at LO, the coherent photoproduction cross section is proportional to the square of the gluon density in the target hadron. The

* Presented at the Cracow Epiphany Conference on Advances in Heavy Ion Physics, Kraków, Poland, January 8–11 2019.

acceptance coverage of the LHC experiments corresponds to a Bjorken-x range from $\sim 10^{-2}$ to $\sim 10^{-5}$, while the heavy-quark mass serves as a hard scale justifying perturbative calculations.

2. Heavy vector meson photoproduction in *pp* and *p*–Pb UPC

Exclusive quarkonium photoproduction off protons in pp collisions and p–Pb UPC can be used to probe the poorly known behavior of the gluon density at low Bjorken-x down to 10^{-5} and search for gluon saturation effects. Exclusive J/ψ photoproduction off protons has been measured in pp collisions by LHCb and in p–Pb collisions by ALICE extending the explored range of γp center-of-mass energies to the TeV scale [3–5] as shown in Fig. 1. The energy dependence of the photoproduction cross section is compatible with a power law showing no significant change in the gluon density behavior down to $x \sim 10^{-5}$ at $Q^2 \sim \frac{1}{4}m^2_{J/\psi}$.

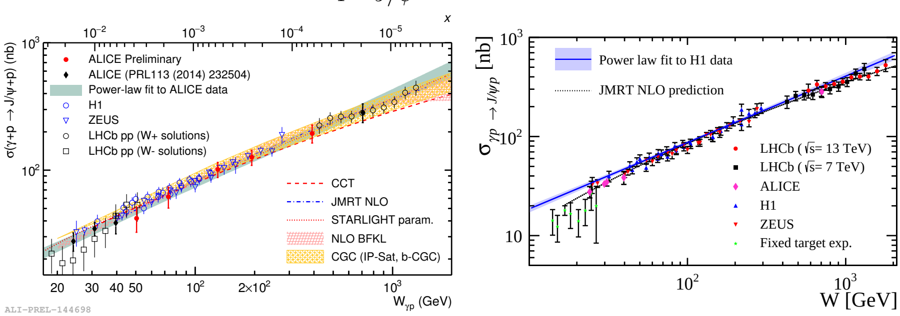

Fig. 1. Cross section of exclusive J/ψ photoproduction off protons as a function of the center-of-mass energy of the photon–proton system measured by ALICE in p–Pb collisions at $\sqrt{s_{NN}} = 5.02$ TeV [5] (left) and measured by LHCb in pp collisions at $\sqrt{s} = 7$ and $\sqrt{s} = 13$ TeV (right) compared to HERA data and theoretical models [6].

Measurements of $\psi(2S)$ or Υ photoproduction would allow one to probe gluon densities at larger Q^2 values. The $\psi(2S)$ and $\Upsilon(1S)$ photoproduction cross sections measured by LHCb in pp collisions [3, 6] and $\Upsilon(1S)$ photoproduction cross sections measured by CMS in p–Pb collisions [7] are compatible with a power-law growth of gluon densities, however, the comparison of Υ measurements with theory calculations indicate the importance of NLO effects [8] as shown in Fig. 2.

In 2016, the ALICE Collaboration measured the J/ψ photoproduction in p–Pb UPC collisions at $\sqrt{s_{NN}} = 8.16$ TeV, see invariant mass distributions for dimuon pairs at forward and backward rapidities in Fig. 3. This sample will allow ALICE to extend the J/ψ photoproduction measurements to the TeV scale.

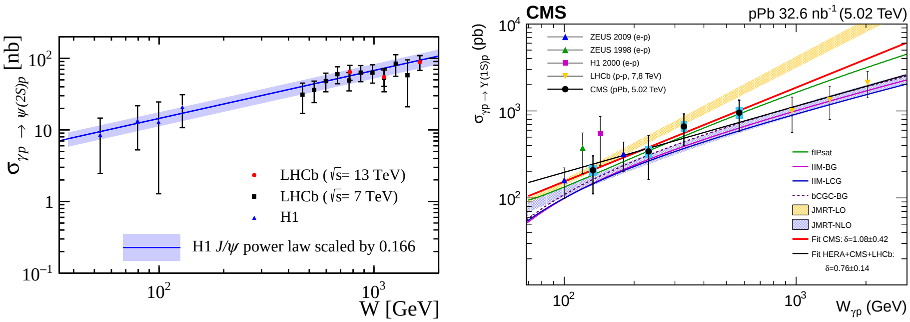

Fig. 2. Cross section of exclusive $\psi(2S)$ (left) and $\Upsilon(1S)$ (right) photoproduction off protons as a function of the center-of-mass energy of the photon–proton system measured by LHCb in pp collisions at $\sqrt{s} = 7$ and $\sqrt{s} = 13$ TeV [6] (left) and by CMS in p–Pb collisions at $\sqrt{s_{NN}} = 5.02$ TeV [7, 9].

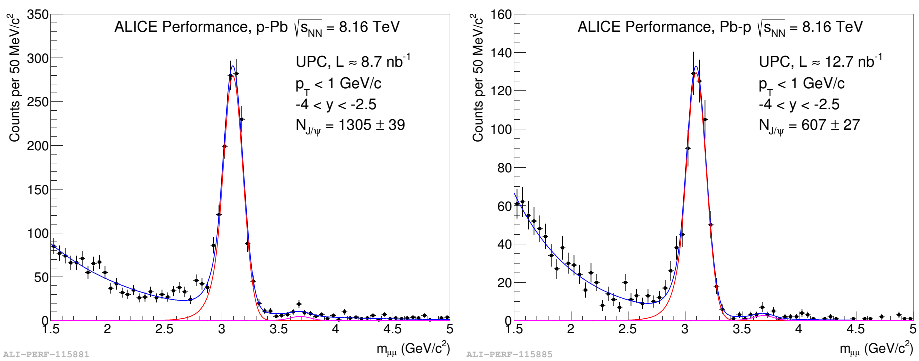

Fig. 3. Invariant mass distributions for unlike-sign dimuons with pair $p_{\mathrm{T}} < 1$ GeV/c and rapidity $-4 < y < -2.5$ in ultra-peripheral p–Pb (left) and Pb–p (right) collisions at $\sqrt{s_{NN}} = 8.16$ TeV, corresponding to γp center-of-mass energy ranges $27 < W_{\gamma p} < 57$ GeV and $700 < W_{\gamma p} < 1480$ GeV, respectively.

3. Charmonium photoproduction in Pb–Pb UPC

Coherent quarkonium photoproduction in Pb–Pb UPC provides a direct tool to study nuclear gluon shadowing effects [10], which are poorly known and play a crucial role in the initial stages of heavy-ion collisions. First ALICE and CMS results from Run 1 on the coherent J/ψ photoproduction cross section in Pb–Pb UPC at $\sqrt{s_{NN}} = 2.76$ TeV are shown in Fig. 4, left [11–13]. The measured cross section is in good agreement with models based on the moderate gluon shadowing from the EPS09 global fit.

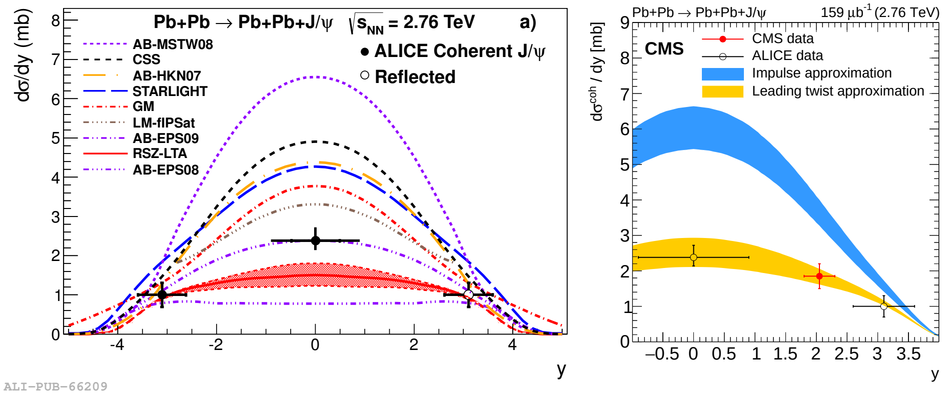

Fig. 4. Coherent J/ψ photoproduction cross section in Pb–Pb UPC at $\sqrt{s_{NN}} = 2.76$ TeV measured by ALICE [12] (left) and CMS [13] (right).

ALICE also published first preliminary results on J/ψ photoproduction in Pb–Pb UPC at $\sqrt{s_{NN}} = 5.02$ TeV from Run 2. The obtained coherent J/ψ yield at forward rapidity is by a factor 50 higher compared to Run 1 results [11] thanks to much higher integrated luminosity, improved trigger logic, wider rapidity range and increased beam energy, see Fig. 5, left. The transverse momentum distribution for dimuons around the J/ψ mass includes several contributions as illustrated in Fig. 5, right. Coherent J/ψ photoproduction, when a photon interacts coherently with the whole nucleus, is characterized by a narrow transverse momentum distribution

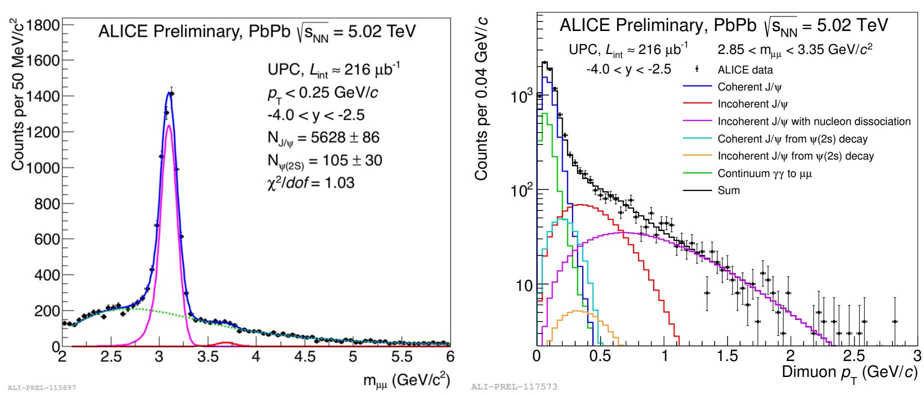

Fig. 5. Left: Invariant mass distribution for unlike-sign dimuons with pair $p_{\mathrm{T}} <$ 0.25 GeV$/c$ and rapidity $-4.0 < y < -2.5$ in ultra-peripheral Pb–Pb collisions at $\sqrt{s_{NN}} = 5.02$ TeV. Right: Transverse momentum distribution for unlike-sign dimuons around J/ψ mass fitted summing six different Monte Carlo templates produced using the STARlight event generator [15].

with $\langle p_{\rm T}\rangle \sim 60$ MeV/c. In the incoherent case, the photon couples to a single nucleon. If the target nucleon stays intact, the charmonium $p_{\rm T}$ distribution is driven by the nucleon form factor, resulting in $\langle p_{\rm T}\rangle \sim 400$ MeV/c. The J/ψ photoproduction on a single nucleon can also be accompanied by nucleon dissociation resulting in a high-$p_{\rm T}$ tail that was fitted with the H1 parameterization [14]. Contributions from continuum dimuon production and feed-down from $\psi(2S)$ decays were also taken into account in the fits. The resulting coherent J/ψ photoproduction cross section at forward rapidity in ultra-peripheral Pb–Pb collisions at $\sqrt{s_{NN}} = 5.02$ TeV is compared to several theoretical predictions in Fig. 6, left.

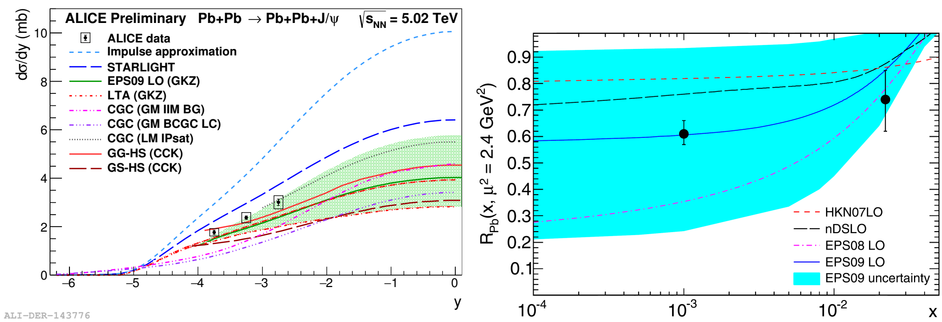

Fig. 6. Left: Measured coherent differential cross section of J/ψ photoproduction in ultra-peripheral Pb–Pb collisions at $\sqrt{s_{NN}} = 5.02$ TeV. Right: Gluon shadowing factor extracted from the ALICE measurements at $\sqrt{s_{NN}} = 2.76$ TeV [10].

The ALICE Collaboration results on coherent J/ψ photoproduction at $\sqrt{s_{NN}} = 5.02$ TeV were used to extract the gluon shadowing factor [10], see Fig. 6, right, indicating that coherent charmonium photoproduction in Pb–Pb UPC may serve as a promising tool to constrain gluon shadowing uncertainties. The ALICE Collaboration also collected a factor 5 higher statistics for J/ψ at central rapidity compared to Run 1 results. Invariant mass distributions for the opposite sign dimuon pairs with their $p_{\rm T} < 0.2$ GeV/c are shown in Fig. 7, left. The coherent J/ψ signal has been also observed in the $p\bar{p}$ channel, see Fig. 7, right. These mid-rapidity results will provide further constraints on the nuclear gluon shadowing at $x \sim 10^{-3}$.

The ALICE experiment also measured the coherent $\psi(2S)$ cross section at mid-rapidity via the dilepton (l^+l^-) decay and in the channel $\psi(2S) \to J/\psi + \pi^+\pi^-$ followed by $J/\psi \to l^+l^-$ decay [16]. The measured coherent $\psi(2S)$ photoproduction cross section, shown in Fig. 8, disfavors models with no nuclear effects and those with strong gluon shadowing, however, different predictions rely on different reference $\gamma + p \to \psi(2S) + p$ cross sections, thus preventing stronger conclusions. Many uncertainties on the measurement and on the γp reference cancel in the ratio of the coherent $\psi(2S)$ and J/ψ

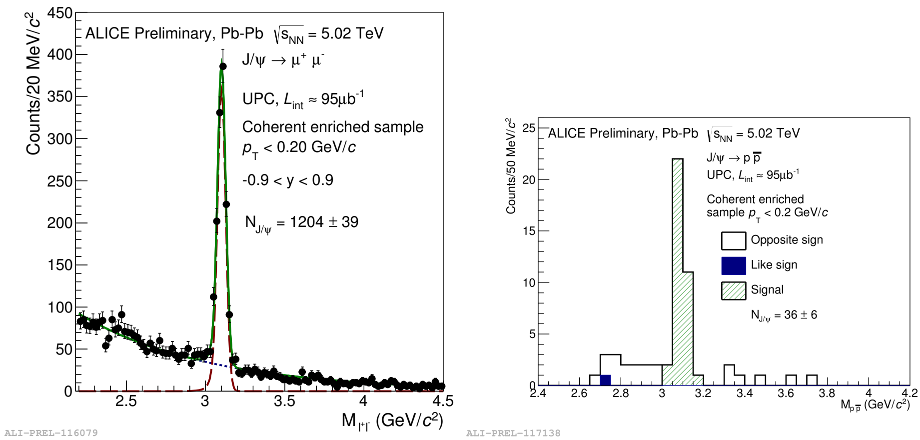

Fig. 7. Invariant mass distribution for unlike-sign dimuons (left) and diprotons (right) with pair $p_{\rm T} < 0.2$ GeV$/c$ and rapidity $|y| < 0.9$ in ultra-peripheral Pb–Pb collisions at $\sqrt{s_{NN}} = 5.02$ TeV.

cross sections. Surprisingly, the measured ratio $\sigma^{\rm coh}_{\psi(2S)}/\sigma^{\rm coh}_{J/\psi} = 0.344^{+0.076}_{-0.074}$ appears to be by a factor two larger than in γp measurements at HERA [17] indicating that nuclear effects may affect differently $1S$ and $2S$ charmonium states.

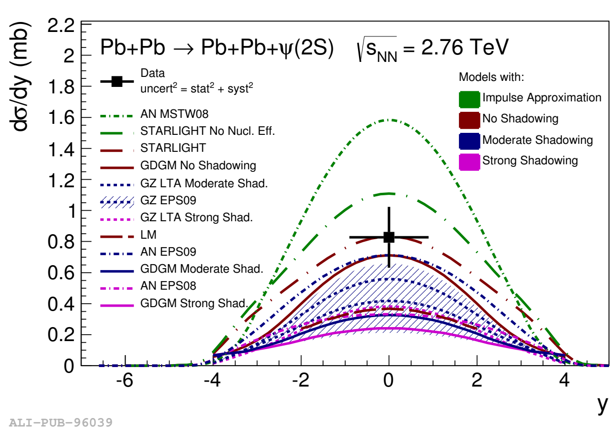

Fig. 8. ALICE results on coherent $\psi(2S)$ photoproduction cross section in Pb–Pb collisions at $\sqrt{s_{NN}} = 2.76$ TeV in comparison with model predictions [16].

ALICE also measured a $\psi(2S)$ signal in $\psi(2S) \to \mu^+\mu^-\pi^+\pi^-$ and $\psi(2S) \to e^+e^-\pi^+\pi^-$ decay channels in Pb–Pb UPC at $\sqrt{s_{NN}} = 5.02$ TeV, as shown in Fig. 9. The experimental uncertainty of these measurements will be significantly improved with a much better statistics expected in Run 3 and 4.

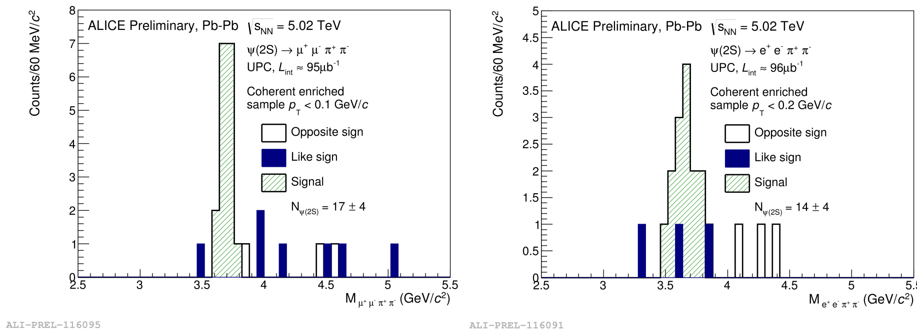

Fig. 9. Invariant mass distributions for $\psi(2S) \rightarrow \mu^+\mu^-\pi^+\pi^-$ and $\psi(2S) \rightarrow e^+e^-\pi^+\pi^-$ decays collected by ALICE in Pb–Pb UPC at $\sqrt{s_{NN}} = 5.02$ TeV.

High statistics data in Run 3 and 4 may also help to decouple low-x and high-x contributions in vector meson production cross sections measured in UPC using differential cross section measurements with and without additional neutron activity in Zero Degree Calorimeters [18]. The expected experimental uncertainties in Run 3 and 4 were evaluated in [19] in terms of the nuclear suppression factor R_{Pb} which is defined as a root square of the ratio of photoproduction cross section $\sigma_{\gamma\mathrm{Pb}}$ measured in Pb–Pb UPC and photoproduction cross section in the Impulse Approximation σ_{IA} calculated as a reference photoproduction cross section off proton scaled by the integral over squared Pb form factor [10]

$$R_{\mathrm{Pb}}(x) = \left(\frac{\sigma_{\gamma\mathrm{Pb}}(x)}{\sigma_{\mathrm{IA}}(x)}\right)^{1/2}, \qquad \text{where} \qquad x = \frac{m_{\mathrm{V}}}{\sqrt{s_{NN}}}\exp(-y)\,, \tag{1}$$

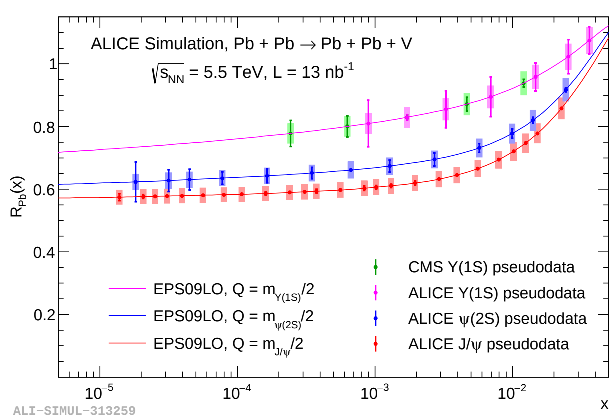

Fig. 10. Pseudodata projections for the nuclear suppression factor measured with heavy vector photoproduction in Pb–Pb UPC collisions at different scales [19].

where $m_{\rm V}$ and y are the mass and rapidity of the produced vector meson. Under the assumption that the coherent photoproduction cross section is proportional to the squared gluon density at the scale $Q = m_{\rm V}/2$, this nuclear suppression factor can be used to constrain nuclear shadowing at different scales. The resulting pseudodata projections, based on EPS09 LO central values, are shown in Fig. 10.

4. J/ψ photoproduction in peripheral Pb–Pb collisions

Although photon-induced reactions are typically measured in UPCs, they have also been observed in hadronic collisions of heavy ions. A strong excess in the yield of J/ψ at forward rapidities at very low transverse momenta $p_{\rm T} < 0.3$ GeV$/c$, measured by ALICE in peripheral Pb–Pb collisions at $\sqrt{s_{NN}} = 2.76$ TeV, results in a large nuclear modification factor $R_{AA} \sim 7$ in this $p_{\rm T}$ range [20]. A similar excess has also been observed by ALICE for J/ψ at central and forward rapidity in peripheral Pb–Pb collisions at $\sqrt{s_{NN}} = 5.02$ TeV [21], see Fig. 11. This excess is commonly interpreted as a signal of coherent J/ψ photoproduction off heavy-ion remnants, see *e.g.* [22, 23].

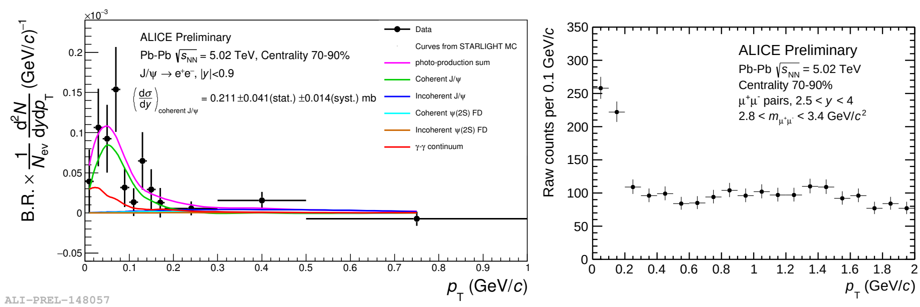

Fig. 11. Transverse momentum spectrum for J/ψ at central rapidity (left) and forward rapidity (right) in peripheral Pb–Pb collisions at $\sqrt{s_{NN}} = 5.02$ TeV [21].

5. Conclusions

Vector meson photoproduction in ultra-peripheral collisions at the LHC has shown to be particularly useful as a probe of proton and nuclear structure. The ALICE, CMS and LHCb results on the exclusive J/ψ photoproduction off protons in pp and p–Pb collisions indicate no significant change in the power-law x dependence of the gluon density in the proton between the HERA and LHC energies. The ALICE and CMS results on the coherent J/ψ photoproduction in ultra-peripheral Pb–Pb collisions are in good agreement with models based on the moderate gluon shadowing from the EPS09 global fit. The ratio of coherent $\psi(2S)$ and J/ψ photoproduction cross sections measured by ALICE indicates that nuclear effects may affect differently $1S$ and $2S$ charmonium states. Last but not least, ALICE observed a surprising excess of J/ψ at low transverse momentum in peripheral Pb–Pb collisions that is commonly interpreted as a signal of coherent J/ψ photoproduction off heavy-ion remnants. The upcoming high-luminosity LHC era will bring much more precise measurements and hopefully new exciting discoveries in photon-induced physics.

REFERENCES

[1] A.J. Baltz, *Phys. Rep.* **458**, 1 (2008) [arXiv:0706.3356 [nucl-ex]].
[2] J.G. Contreras, J.D. Tapia Takaki, *Int. J. Mod. Phys. A* **30**, 1542012 (2015).
[3] LHCb Collaboration, LHCb-CONF-2016-007 (2016).
[4] B.B. Abelev *et al.* [ALICE Collaboration], *Phys. Rev. Lett.* **113**, 232504 (2014) [arXiv:1406.7819 [nucl-ex]].
[5] ALICE Collaboration, arXiv:1809.03235 [nucl-ex].
[6] R. Aaij *et al.* [LHCb Collaboration], *J. High Energy Phys.* **1810**, 167 (2018).
[7] A.M. Sirunyan *et al.* [CMS Collaboration], *Eur. Phys. J. C* **79**, 277 (2019) [arXiv:1809.11080 [hep-ex]].
[8] S.P. Jones, A.D. Martin, M.G. Ryskin, T. Teubner, *J. Phys. G* **43**, 035002 (2016) [arXiv:1507.06942 [hep-ph]].
[9] R. Aaij *et al.* [LHCb Collaboration], *J. High Energy Phys.* **1509**, 084 (2015) [arXiv:1505.08139 [hep-ex]].
[10] V. Guzey, E. Kryshen, M. Strikman, M. Zhalov, *Phys. Lett. B* **726**, 290 (2013) [arXiv:1305.1724 [hep-ph]].
[11] B. Abelev *et al.* [ALICE Collaboration], *Phys. Lett. B* **718**, 1273 (2013) [arXiv:1209.3715 [nucl-ex]].
[12] E. Abbas *et al.* [ALICE Collaboration], *Eur. Phys. J. C* **73**, 2617 (2013) [arXiv:1305.1467 [nucl-ex]].
[13] V. Khachatryan *et al.* [CMS Collaboration], *Phys. Lett. B* **772**, 489 (2017) [arXiv:1605.06966 [nucl-ex]].
[14] C. Alexa *et al.* [H1 Collaboration], *Eur. Phys. J. C* **73**, 2466 (2013) [arXiv:1304.5162 [hep-ex]].
[15] S.R. Klein *et al.*, *Comput. Phys. Commun.* **212**, 258 (2017) [arXiv:1607.03838 [hep-ph]].
[16] J. Adam *et al.* [ALICE Collaboration], *Phys. Lett. B* **751**, 358 (2015) [arXiv:1508.05076 [nucl-ex]].
[17] C. Adloff *et al.*, *Phys. Lett. B* **541**, 251 (2002) [arXiv:hep-ex/0205107].
[18] V. Guzey, M. Strikman, M. Zhalov, *Eur. Phys. J. C* **74**, 2942 (2014) [arXiv:1312.6486 [hep-ph]].

[19] Z. Citron *et al.*, arXiv:1812.06772 [hep-ph].

[20] J. Adam *et al.* [ALICE Collaboration], *Phys. Rev. Lett.* **116**, 222301 (2016) [arXiv:1509.08802 [nucl-ex]].

[21] L. Massacrier, arXiv:1902.03637 [hep-ex].

[22] J. Cepila, J.G. Contreras, M. Krelina, *Phys. Rev. C* **97**, 024901 (2018) [arXiv:1711.01855 [hep-ph]].

[23] W. Zha *et al.*, *Phys. Rev. C* **97**, 044910 (2018) [arXiv:1705.01460 [nucl-th]].